An Alternative One-Diode Model for Illuminated Solar Cells

Otwin Breitenstein

Abstract—A novel one-diode model is proposed for illuminated solar cells, which contains an additional variable resistance describing minority carrier diffusion from the bulk to the p-n junction. This model naturally describes the differences between photo- and electroluminescence imaging, as well as a well-known departure from the superposition principle.

Index Terms—Electroluminescence (EL) imaging, one-diode model, photoluminescence (PL) imaging, solar cell modeling, superposition principle.

I. INTRODUCTION

HE well-accepted model describing a simple solar cell is the one-diode model containing a series resistance; see Fig. 1. If recombination in the depletion layer plays a role, and/or if ohmic shunts are present, parallel to the diode in Fig. 1(a), second diode and/or a parallel resistance may be added, leading to the two-diode model. Although the values of the parameters of this model may substantially differ between the classical diode theory and experimental reality, which holds, in particular for industrial multicrystalline silicon solar cells, the reasons for these discrepancies are basically well understood [1]. In the following, only the one-diode model will be considered. In this model, the current J_d through the diode represents the dark current due to recombination in the bulk and at the surfaces, described by the saturation current density J_{01} . Under low injection condition, the ideality factor of this diode current is unity, as long as the minority carrier lifetime is constant. Within this model, the voltage at the diode V_{loc} represents the local voltage at the p-n junction, which is given by the terminal voltage V modified by the voltage drop at the series resistance R_s due to the terminal current J. Since the diode in Fig. 1 itself is not illuminated, the physical meaning of $V_{\rm loc}$ is the implied voltage in the bulk of this diode; hence, the separation of the quasi-Fermi levels for electrons and holes divided by the electron charge q. Only then the diode current can be described by the well-known diode formula $J_d = J_{01} \exp(V_{loc}/V_T)$. For V=0 (short-circuit condition), the constant current source $J_{\rm sc}$ represents the short-circuit current of this cell. Physically, $J_{\rm sc}$ corresponds to the total amount of photogenerated carriers times the collection probability. One implication of this model is that, for $R_s = 0$, the implied voltage equals the terminal voltage, both with and without illumination. Another implication is that,

Manuscript received November 5, 2013; accepted February 27, 2014. Date of publication March 24, 2014; date of current version April 18, 2014.

The author is with the Max Planck Institute of Microstructure Physics, 06120 Halle, Germany (e-mail: breiten@mpi-halle.de).

Digital Object Identifier 10.1109/JPHOTOV.2014.2309796

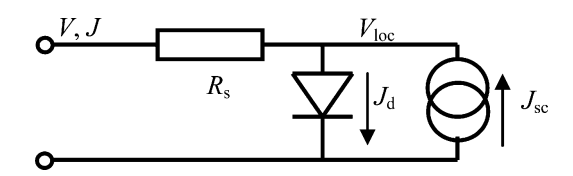


Fig. 1. Conventional one-diode model of an illuminated solar cell.

for $R_s=0$, the superposition principle holds; hence, the device current under illumination J equals that in the dark reduced by $J_{\rm sc}$.

While this model is able to interpret, e.g., electroluminescence (EL) imaging experiments, it cannot describe photoluminescence (PL) imaging experiments correctly. It was pointed out by Trupke $et\ al.$ [2] that, for interpreting PL images, from each image taken at a certain voltage V, an image taken under short-circuit condition at the same illumination intensity has to be subtracted. This measure compensates for luminescence due to "diffusion-limited carriers." Hence, for voltages significantly lower than the open-circuit voltage $V_{\rm oc}$, the concentration of minority carriers in the bulk is under illumination substantially higher than in the dark, which cannot be described in the frame of the one-diode model of Fig. 1.

Moreover, it was shown by Robinson et al. [3], based on PC1D simulations, that there is one type of departure from the superposition principle called departure 2 in [3], which also cannot be described by the one-diode model of Fig. 1. This departure occurs in any type of solar cells showing bulk recombination, even if the lifetime is independent of the carrier concentration. Here, the illuminated current reduced by $J_{\rm sc}$, in the low forward bias region below 0.5 V, is larger than the dark current. This appears like an additional parallel resistance and/or second diode current contribution, which only exist under illumination but not in the dark. Indeed, the magnitude of this effect was shown to depend on the illumination intensity; hence, the departure becomes lower with lower intensity. It was explained in [3] that this effect is the result of a bias-dependent modification of the carrier concentrations across the p-n junction depletion region, which is different under illumination from that in the dark. In addition, this effect cannot be described in the frame of the one-diode model of Fig. 1.

In this contribution, based on PC1D (a popular 1-D solar cell simulation tool; see [4]) simulations of an idealized solar cell, an alternative one-diode model of illuminated solar cells is introduced, which, already in its simplest form, may describe naturally the differences between EL and PL imaging. If it is considered that under illumination, the recombination volume is slightly bias-dependent; in addition, the departure 2 from the superposition principle can be explained by this model.

TABLE I PC1D SOLAR CELL PARAMETERS

Quantity	Value
cell thickness	200 μm
base doping concentration	1.5*10 ¹⁶ cm ⁻³
S front	10^{6} cm/s
S back	10^5 cm/s
bulk lifetime	30 μs
temperature	25 °C

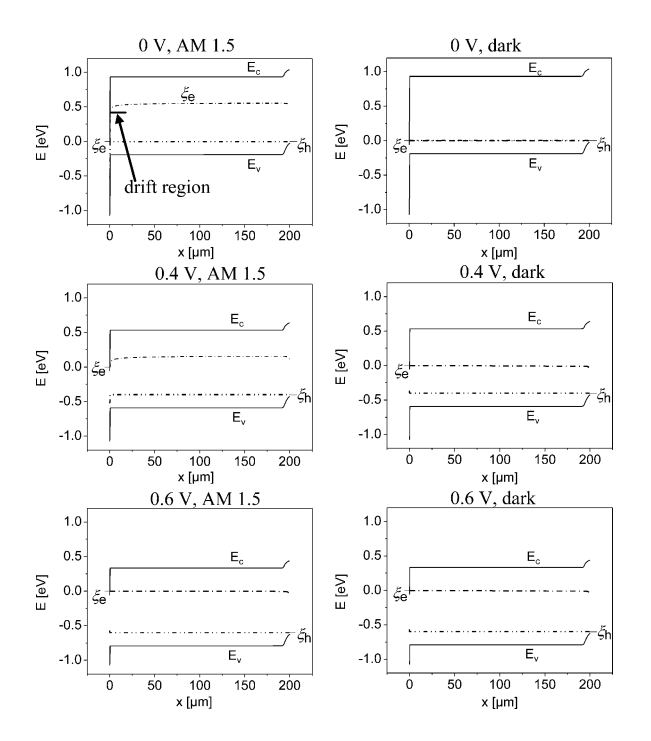


Fig. 2. Band diagrams under various biases under AM 1.5 illumination and in the dark ($E_c=$ conduction band edge, $E_v=$ valence band edge, $\xi_e=$ electron quasi-Fermi level, $\xi_h=$ hole quasi-Fermi level).

II. PC1D SIMULATIONS

Since in this contribution only basic physical principles of a solar cell will be described, the PC1D simulations [4] were performed on a slightly idealized solar cell model. Table I shows the main parameters of this model, which is based on the "Pvcell_15%.prm" example in [4], describing a standard industrial solar cell. For getting rid of any series resistance effects, the contact resistances and the base circuit resistances have been chosen close to zero. The parallel resistance was disabled, the cell thickness was reduced to 200 $\mu \rm m$, and the bulk lifetime was chosen to be 30 $\mu \rm s$. All other parameter has remained as in the example. By these measures, the efficiency at AM 1.5 has increased from 15 to 16.5% at $V_{\rm oc}=0.602$ V.

Fig. 2 shows the bands and the positions of the quasi-Fermi levels across this device simulated by PC1D for three voltages under illumination at AM 1.5 (left) and in the dark (right). The very thin emitter is lying at the left edge; the kink at the right edge is due to the back surface field region. While in the dark the electron (minority carrier) quasi-Fermi level crosses the bulk nearly horizontally for all biases, under illumination and $V < V_{\rm oc}$, the

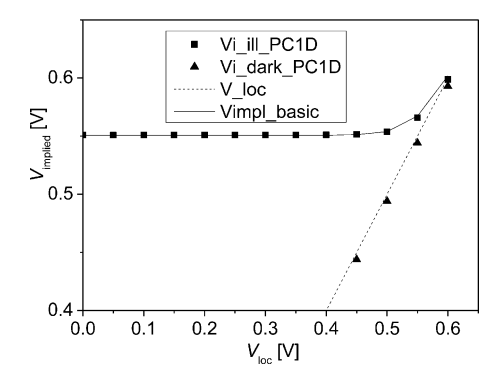


Fig. 3. Implied voltage in the bulk as a function of the local voltage at the p-n junction, simulated by PC1D under 1.5 sun illumination (squares) and in the dark (triangles), in comparison with $V_{\rm loc}$ and the basic analytic simulation under illumination (see Section III-A.).

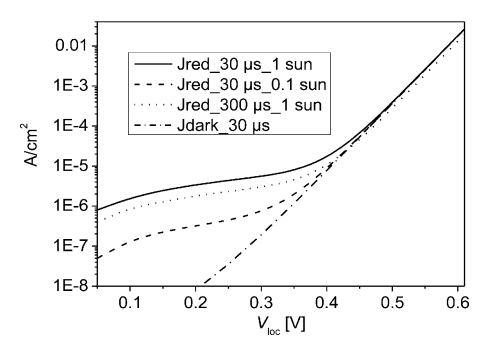


Fig. 4. PC1D simulated dark and illuminated characteristics (reduced by $J_{\rm sc})$ for various parameters.

electron Fermi level in the bulk is lying significantly above that in the emitter. Fig. 3 shows the dependence of the implied voltage in the middle of the bulk, which is the distance between the two quasi-Fermi levels in this position divided by the electron charge q, under illumination and in the dark, as a function of the local junction voltage $V_{\rm loc}$. In the dark, the implied voltage nicely follows the local voltage at the p-n junction, as expected by the equivalent circuit of Fig. 1, just reduced by a few millivolt due to the finite diffusion length in the bulk. Under illumination, on the other hand, over a wide bias range from zero to about 0.45 V, the implied voltage stays nearly constant at about 0.55 V and only beyond approaches $V_{\rm loc}$. Under $V_{\rm oc}$ condition (here, $V_{\rm loc} = 0.602$ V), the implied voltages under illumination and in the dark nearly coincide. Finally, Fig. 4 shows three simulated illuminated I-V characteristics (reduced by their respective J_{sc}) for various parameters in comparison with one dark characteristic. The departure from the superposition principle described by Robinson et al. [3] is clearly visible. Although there was no parallel resistance used in the PC1D simulation, the illuminated characteristic for 30 μ s and 1 sun can be fitted [5] by $J_{01} =$ 1.3×10^{-12} A/cm² (same as for the dark characteristic), $R_p =$ 58 k Ω cm² (infinite for dark), and a second diode contribution of $J_{02} = 1.2 \times 10^{-8} \text{A/cm}^2$ with $n_2 = 3.4$, which are both significantly larger than in the dark. Increasing the lifetime and reducing the illumination intensity reduces the departure effect.

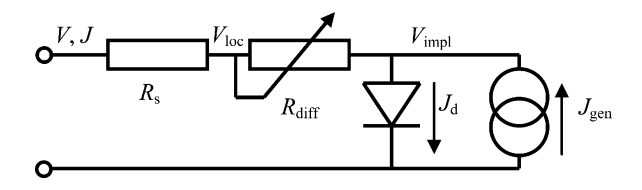


Fig. 5. Proposed equivalent circuits of an illuminated solar cell with the diffusion resistance $R_{\rm diff}$ described by a variable resistance.

III. ALTERNATIVE SOLAR CELL MODEL

In the following, only the bulk part of the first diode current is considered, which corresponds to the p-doped base of a conventional solar cell. Similar considerations also hold for the emitter. The basic idea for the model is to consider the bulk as a reservoir for minority carriers, which are spread there relatively homogeneous, as it was also considered, e.g., in the analytic solar cell model of Cuevas [6]. In contrast with [6], however, here the cell current is described as a diffusion process between the bulk and the p-n junction.

A. Basic Model

Fig. 5 shows the equivalent circuit for the proposed model. This model distinguishes between the local junction voltage at the p-n junction $V_{\rm loc}$ and the local implied voltage in the bulk $V_{\rm impl}$. In this model, a variable diffusion resistance $R_{\rm diff}$ describes the voltage drop between $V_{\rm impl}$ and $V_{\rm loc}$, whereby the resistance depends on the bias. Under forward bias, this diffusion resistance becomes negligibly small, and this equivalent circuit reduces to that in Fig. 1. For low forward bias under illumination, this diffusion resistance essentially acts as a constant current source.

In this model, the constant current source not only describes the short-circuit current $J_{\rm sc}$ but the total amount of carriers $J_{\rm gen}$ generated by absorption in the bulk. The difference between these two currents is the current $J_{\rm rec,0}$, which is the current loss due to recombination in the bulk at $V_{\rm loc} = 0$ V

$$J_{\text{gen}} = J_{\text{sc}} + J_{\text{rec 0}}.\tag{1}$$

In the following, only the "local diode" characterized by an applied voltage of $V_{\rm loc}$ will be treated, since the inclusion of the conventional series resistance R_s would considerably complicate the treatment. Afterwards, an influence of a series resistance can easily be regarded. Here, the "local diode" consists from the actual diode describing the recombination in the bulk, the constant current source $J_{\rm gen}$ describing the total amount of absorbed carriers, and the variable diffusion resistance $R_{\rm diff}$. This basic model assumes that the electron concentration at the edge of the p-n junction to the bulk $n_{\rm pn}$ is also under illumination given by the local voltage

$$n_{\rm pn} = \frac{n_{\rm i}^2}{N_{\rm A}} \exp\left(\frac{V_{\rm loc}}{V_{\rm T}}\right) \tag{2}$$

 $(V_T = \text{thermal voltage}, n_i = \text{intrinsic carrier concentration}, N_A = \text{net acceptor concentration})$. In analogy, the electron con-

centration in the bulk is given by

$$n_{\text{bulk}} = \frac{n_{\text{i}}^2}{N_{\text{A}}} \exp\left(\frac{V_{\text{impl}}}{V_{\text{T}}}\right).$$
 (3)

The recombination rate in the bulk, expressed as a current density, is given for $V_{\rm impl} \gg V_T$ by

$$J_{\rm rec}\left(V_{\rm impl}\right) = J_{01} \exp\left(\frac{V_{\rm impl}}{V_{\rm T}}\right) \tag{4}$$

with J_{01} being the saturation current density describing the dark I–V characteristic. Note that, according to Fig. 2, in the dark, $V_{\rm loc} = V_{\rm impl}$ holds. According to this model, the cell current J can be described by the difference of the electron concentrations, (3) and (2), multiplied by a formal effective diffusion coefficient $D_{\rm eff}$. On the other hand, the cell current equals the difference between the generation and the bulk recombination current densities, which lead to

$$J = D_{\text{eff}} \left(n_{\text{bulk}} - n_{\text{pn}} \right) = J_{\text{gen}} - J_{01} \exp \left(\frac{V_{\text{impl}}}{V_{\text{T}}} \right).$$
 (5)

Of course, assuming a constant effective diffusion coefficient, independent from the applied bias, there is an approximation, which is made here for the sake of convenience. For $V_{\rm loc}=0$ (short circuit), the bulk recombination current equals $J_{\rm rec,0}$. Note that, according to the simulations in Fig. 2, even in this case, $V_{\rm impl}$ is significantly larger than zero. This voltage may be calculated after (4) as

$$V_{\rm impl}^0 = V_{\rm T} \ln \left(\frac{J_{\rm rec,0}}{J_{01}} \right). \tag{6}$$

This allows to calculate the effective diffusion coefficient from the knowledge of $J_{\rm sc}$ and $J_{{\rm rec},0}$

$$D_{\text{eff}} \left(n_{\text{bulk}}^0 - n_{\text{pn}}^0 \right) = J_{\text{sc}} = D_{\text{eff}} \left(\frac{n_i^2 J_{\text{rec},0}}{N_{\text{A}} J_{01}} - \frac{n_i^2}{N_{\text{A}}} \right). \tag{7}$$

Since the last term in the bracket in (7) can be neglected, this leads to

$$D_{\text{eff}} = \frac{J_{\text{sc}} J_{01} N_{\text{A}}}{n_{\text{i}}^2 J_{\text{rec},0}}.$$
 (8)

If (8) is inserted into (5), this leads, together with (1)–(3), to the following analytic expression for V_{impl} :

$$V_{\rm impl}(V_{\rm loc}) = V_{\rm T} \ln \left(\frac{J_{\rm rec,0}}{J_{01}} + \frac{J_{\rm sc}}{J_{\rm gen}} \exp \left(\frac{V_{\rm loc}}{V_{\rm T}} \right) \right). \tag{9}$$

For the values of $J_{\rm sc}=32.9~{\rm mA/cm^2}$ and $J_{01}=1.3\times 10^{-12}{\rm A/cm^2}$ of our PC1D model cell, the data in Fig. 3 can nicely be fitted by this formula by assuming $J_{\rm rec,0}=3.65~{\rm mA/cm^2}$, which is about 8% of $J_{\rm sc}$. In this case, (8) leads to a value of $D_{\rm eff}=3.28\times 10^{-15}{\rm Acm}$.

If (9) is inserted into (5), the illuminated characteristic of the local diode can be calculated as $J(V_{\rm loc}) = J_{\rm gen} - J_{\rm rec}(V_{\rm loc})$. Interestingly, it can be shown analytically that the result is a simple exponential characteristic

$$J(V_{\rm loc}) = J_{\rm sc} - \frac{J_{\rm sc}}{J_{\rm gen}} J_{01} \exp\left(\frac{V_{\rm loc}}{V_{\rm T}}\right). \tag{10}$$

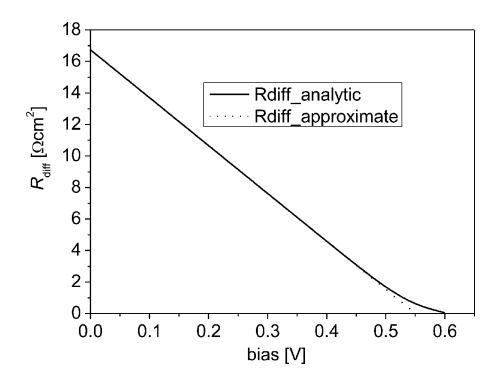


Fig. 6. Analytic and approximate dependence of $R_{\rm diff}$ on $V_{\rm loc}$ for the chosen model parameters.

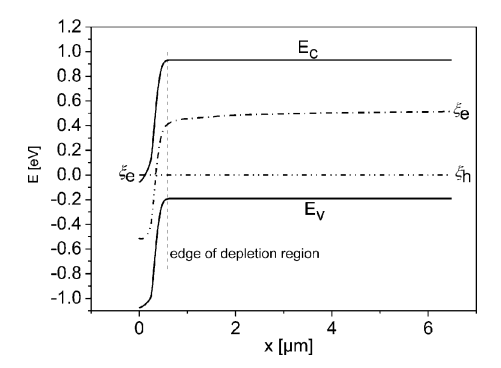


Fig. 7. Band diagram near the p-n junction at 0 V under illumination.

This means that the alternative model introduced here leads to the same illuminated characteristic as the conventional one does. The factor $J_{\rm sc}/J_{\rm gen}$ in front of J_{01} accounts for the fact that, according to Fig. 5, the open circuit is established by the balance of J_d and $J_{\rm gen}$ and not by the balance of J_d and $J_{\rm sc}$, as in Fig. 1. Hence, this basic model does not yet describe the departure from the superposition principle shown in Fig. 4. The slightly reduced value of J_{01} (by a factor of $J_{\rm sc}/J_{\rm gen}$, compared with the dark characteristic) is not verified by the PC1D simulations; see the discussion in Section IV.

Knowing $V_{\rm impl}$ from (9) and J from (10), the bias-dependent value of the variable resistor $R_{\rm diff}$ in Fig. 5(a) may be calculated as

$$R_{\text{diff}}(V_{\text{loc}}) = \frac{V_{\text{T}} \ln \left(\frac{J_{\text{rec},0}}{J_{01}} + \frac{J_{\text{sc}}}{J_{\text{gen}}} \exp \left(\frac{V_{\text{loc}}}{V_{\text{T}}}\right)\right) - V_{\text{loc}}}{J_{\text{sc}} - \frac{J_{\text{sc}}}{J_{\text{gen}}} J_{01} \exp \left(\frac{V_{\text{loc}}}{V_{\text{T}}}\right)}.$$
(11)

Fig. 6 shows this dependence. For low and medium bias, it can be described approximatively by $R_{\rm diff} = (V_{\rm impl}^0 - V_{\rm loc})/J_{\rm sc}$, which is just the rule for a constant current source. If the bias approaches $V_{\rm oc}$, $R_{\rm diff}$ approaches zero.

B. Advanced Model

If the PC1D simulations are thoroughly checked in the region close to the p-n junction, it becomes visible that the assumptions of the basic model are not generally met. Fig. 7 shows the band structure in this region for $V_{\rm loc}=0$ under AM 1.5 illumination. While the hole (majority carrier) quasi-Fermi level goes straight

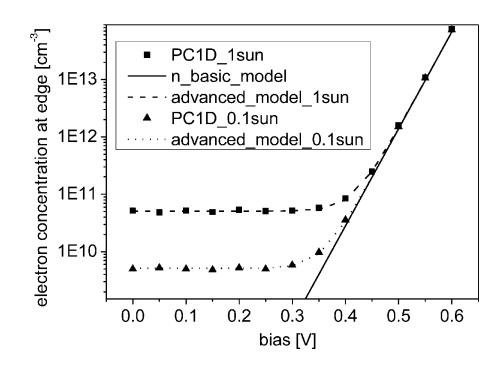


Fig. 8. Electron concentration at the edge of the depletion layer simulated by PC1D for two illumination intensities, together with model predictions.

through the p-side of the depletion region, as expected, it is visible that the electron quasi-Fermi level does not go straight through, as assumed in the basic model. Instead, the electron concentration at the edge of the depletion region is at $V_{\rm loc}=0$, which is significantly higher than predicted by (2). In fact, by PC1D a value of $n_{\rm edge}^0=5.51\times10^{10}~{\rm cm}^{-3}$ is simulated there, which is still a factor of 178 below the maximum bulk concentration of $n_{\rm bulk}^0=9.86\times10^{12}~{\rm cm}^{-3}$ in the center of the bulk. Thus, the general approach of the basic model, that the electron current is driven by a concentration difference between the bulk and the edge of the depletion region, is still true, but the numbers are somewhat different.

This edge electron concentration was simulated by PC1D for various biases and two illumination intensities with the results shown in Fig. 8. Here, the criterion for meeting the edge was that the hole concentration is reduced by 10%. It is visible that the edge electron concentration at low bias does not fall below a certain value, which is proportional to the illumination intensity and, hence, to the flowing current density. This corresponds to a maximum drift velocity $v_{\rm max}$ according to $(q={\rm electron}\, {\rm charge})$:

$$J_{\rm sc} = v_{\rm max} n_{\rm edge} q. \tag{12}$$

The carrier density limits of 5.1×10^{10} and 5.1×10^{9} in Fig. 8 for 1 and 0.1 sun, corresponding to $J_{\rm sc}$ of 32.9 and 3.29 mA/cm², respectively, are compatible with a maximum drift velocity of $v_{\rm max}=4.03\times 10^6$ cm/s. This is already in the order of but still below the thermal velocity at 25 °C. Thus, in the advanced model the electron concentration close to the p-n junction is calculated as

$$n_{\rm pn} = \frac{n_{\rm i}^2}{N_{\rm A}} \exp\left(\frac{V_{\rm loc}}{V_{\rm T}}\right) + \frac{J_{\rm sc}}{v_{\rm max}q}.$$
 (13)

These curves, which nicely fit the PC1D simulations, are also shown in Fig. 8.

The departure from the superposition principle shown in Fig. 4 mainly consists from a weak linear recombination current component at low biases. Fig. 9 shows these data again in linear drawing in the low-current range, together with the characteristic of a 58-k Ω cm² resistor, which was already found in the I-V analysis of the PC1D-generated data. It is visible that, even in this low bias range, the reduced currents are not exactly linear.

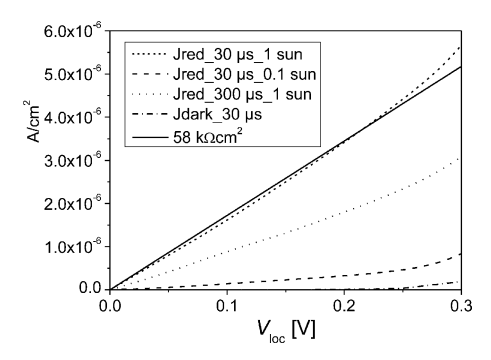


Fig. 9. Low current part of PC1D simulated dark and illuminated characteristics (reduced by $J_{\rm SC}$) for various parameters and pure ohmic curve.

This points to the fact that the departure from superposition not only generates an additional R_p but an additional J_{02} (second diode) contribution as well as it was found already in the diode fit of the data in Fig. 4.

If there is no ohmic parallel resistor, this linear behavior in the low bias range points to a slightly linear dependence of the recombination probability in the bulk from the applied bias in the low bias range, which only acts under illumination. It is proposed here that the major reason for this dependence stems from a slightly bias-dependent recombination volume in the bulk. Under forward bias, in the dark the recombination, volume starts at the edge of the depletion region and basically ends at the back surface field region. Under illumination and low forward bias, the electron concentration close to the depletion region is significantly lower than that in the depth of the bulk; in the discussion of Fig. 7(a), a factor of 178 was found. An evaluation of the electron density profile at 0 V at AM 1.5 has revealed that the local maximum of the electron concentration is close to the center of the bulk ($x = 100 \mu m$) and that this concentration is reduced by a factor of e (the Euler number, corresponding to a lowering of the electron quasi-Fermi level by kT) at a distance of about 22 μ m from the edge of the p-n junction and increasingly further reduces when further approaching the junction. This region may be called the electron drift region showing a significant concentration gradient, where the carrier diffusion described in this contribution essentially takes place. In Fig. 2, this drift region is indicated in the top left image. It can be assumed that, due to the significantly reduced electron concentration in this region, this region does not contribute to the bulk recombination under illumination at low bias. If, according to Fig. 8, the electron concentration at the edge of the junction is constant in the bias range between 0 and 0.3 V, the extension of this electron drift region should be independent of the bias. However, the width of the depletion region slightly changes with bias, which shifts the whole electron drift region, and, thus, modulates the width of the remaining bulk recombination region. Although the degree of this modulation is very tiny, this makes a significant contribution to the shape of the reduced illuminated current, since here, two relatively large currents are subtracted from each other. It had been shown previously that, within the basic model introduced in Section III-A, under idealized conditions (constant recombination vol-

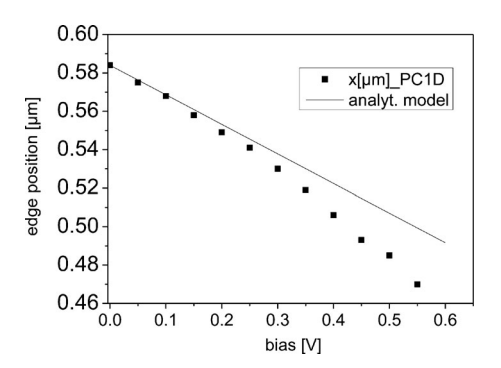


Fig. 10. Edge position of the depletion layer simulated by PC1D and according to the linear model (14).

ume), this difference still leads to an exponential characteristic. If, however, one of these two currents (recombination) shows only a slight additional linear component, this can easily be seen in the half-logarithmic drawing of the reduced current, as will be shown later. The width of the depletion region can be linearized for low forward biases ($V_d = \text{diffusion voltage}$, about 0.9 V), total depletion, and asymmetric junction approximation

$$W(V) = \sqrt{\frac{2\varepsilon\varepsilon_0 (V_{\rm d} - V)}{qN_{\rm A}}} \approx W(0) \left(1 - \frac{V}{2V_{\rm d}}\right). \tag{14}$$

In our case, for $N_A=1.5\times 10^{16}~{\rm cm^{-3}}~W(0)=278~{\rm nm}$ holds, which leads, according to (14), for low voltages, to a dependence of W from V of

$$\frac{\partial W}{\partial V} = -154 \text{ nm/V}. \tag{15}$$

Fig. 10 shows the x-position of the edge of the depletion layer according to PC1D simulations, in comparison with the linear prediction (14) and (15). These data were the same under illumination and in the dark. Again, the criterion for meeting the edge was a reduction of the hole concentration by 10%. For V=0, the linear prediction is nicely met, and for higher voltages, the simulations show the expected nonlinear behavior.

The slightly bias-dependent recombination volume may be expressed in (5) as a bias-dependent value of J_{01} , since J_{01} is a measure of the bulk recombination rate for a given value of $V_{\rm impl}$. Assuming that volume recombination dominates over backside recombination and that a region from the depletion region edge to $d_0 = 22~\mu{\rm m}$ and beyond does not contribute to the bulk recombination under illumination at low bias, $J_{01}(V)$ may be expressed with (15) as $(d={\rm bulk}~{\rm thickness}=200~\mu{\rm m})$

$$J_{01}(V) = J_{01}^{\text{dark}} \frac{d - d_0 + \frac{\partial W}{\partial V} V}{d}.$$
 (16)

This has to be inserted into (9) with regard to the influence of a variable recombination volume on $V_{\rm impl}$ in the advanced model. For correctly meeting the value of $V_{\rm impl}^0 = 0.5508$ V simulated by PC1D, the value of $J_{\rm rec,0}$ has to be reduced for the advanced model from the previous 2.65 mA/cm² to 2.37 mA/cm². This $J_{\rm rec,0}^{\rm adv}$ is just the factor $F = (d-d_0)/d$ smaller than the basic $J_{\rm rec,0}$, by which J_{01} (proportional to the bulk recombination probability) decreases in (16) by the insertion of the

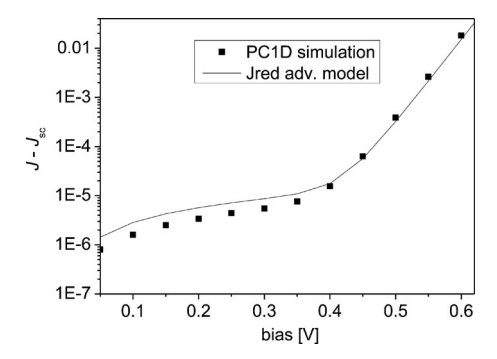


Fig. 11. Illuminated $I\!-\!V$ characteristic reduced by $J_{\rm sc}$ simulated by PC1D and predicted by the advanced solar cell model.

low-recombination drift region. Actually, in the formula for the effective diffusion coefficient (7), the term for $n_{\rm pn}$ now has to be regarded, leading, together with (13) and (16) (for $V_{\rm loc}=0$), to another formula for $D_{\rm eff}$

$$D_{\text{eff}}^{\text{adv}} = \frac{J_{\text{sc}}}{n_{\text{bulk}}(V_{\text{impl}}^{0}) - n_{\text{edge}}} = \frac{J_{\text{sc}}}{\frac{n_{\text{i}}^{2} J_{\text{rec},0}^{\text{adv}} d}{N_{\text{A}} J_{01}^{\text{dark}} (d - d_{0})} - \frac{J_{\text{sc}}}{v_{\text{max}} q}}.$$
(17)

Since the factor F is also contained in $J_{\rm rec,0}^{\rm adv}$, the only difference to (8) is introduction of (13), which is small compared with $n_{\rm bulk}^0$. In our case, $D_{\rm eff}$ increases by this measure only slightly from 3.28×10^{-15} to 3.29×10^{-15} Acm, which is negligible. Thus, from (9) with (17), the final expression for the implied voltage in the advanced model is

$$V_{\rm impl}^{\rm adv}(V_{\rm loc}) =$$

$$V_{\rm T} \ln \left(\frac{J_{\rm rec,0}^{\rm adv}}{J_{01}(d - d_0 + \frac{\partial W}{\partial V} V_{\rm loc})} + \frac{J_{\rm sc}}{J_{\rm gen}} \exp \left(\frac{V_{\rm loc}}{V_{\rm T}} \right) \right). (18)$$

If the correct value of $J_{\rm rec,0}^{\rm adv}$ is used here, this prediction is visually indistinguishable from the prediction of the basic model in Fig. 3. Hence, apart from the different value of $J_{\rm rec,0}$ due to the existence of the low-recombination drift region, the prediction of the implied voltage by the advanced model does not differ significantly to that of the basic model. Therefore, for interpreting PL images, the basic model is sufficient.

However, this does not hold for the prediction of the illuminated current reduced by $J_{\rm sc}$. Again, for calculating the current after the left side of (5), (13) has to be used to calculate $n_{\rm pn}$ instead of (2), together with (3), leading to

$$J(V_{\rm loc}) = D_{\rm eff}^{\rm adv} \frac{n_{\rm i}^2}{N_{\rm A}} \left(\exp\left(\frac{V_{\rm impl}^{\rm adv}}{V_{\rm T}}\right) - \exp\left(\frac{V_{\rm loc}}{V_{\rm T}}\right) - \frac{J_{\rm sc}}{v_{\rm max}q} \right). \tag{19}$$

Fig. 11 shows the result of this advanced analytic model for our cell with $\tau=30~\mu s$ at AM 1.5 in comparison with the PC1D-simulated illuminated and dark characteristic. We see that this model nicely describes the departure from the superposition principle shown in Fig. 4 and described by Robinson *et al.* [3]. The departure is due to a tiny linear dependence of $J_{01}^{\rm adv}$ and by this of $V_{\rm impl}^{\rm adv}$ on $V_{\rm loc}$ in (18) in the low-voltage range. The departure effect is even slightly stronger in the model than in

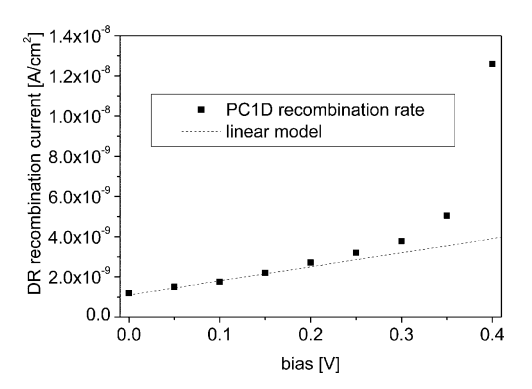


Fig. 12. Recombination current contribution from the p-side of the depletion region simulated by PC1D and according to a linear model.

the PC1D simulation. This may be due to the fact that in (16), it is assumed that bulk recombination dominates. If there is some significant backside recombination, the dependence of J_{01} on V may become weaker.

There is another mechanism that may lead to a linear contribution to the illuminated characteristic, which is recombination in the depletion region. It can be seen in Fig. 7 that, at low voltages, the electron concentration in the right part of the depletion region is significantly higher than expected by the basic model of this study, assuming that the electron quasi-Fermi level crosses the whole depletion layer horizontally. This also increases the recombination rate in the depletion layer, which is proportional to the local p-n product. This effect becomes gradually weaker with increasing bias and vanishes if the electron concentration at the edge approaches that predicted by the basic model; see Fig. 8. In addition, this effect is proportional to the illumination intensity. The cumulative recombination rate in the depletion layer has been calculated by PC1D for various biases under AM 1.5 illumination. Fig. 12 shows the recombination current from the p-side of the depletion region, counted from the mid of the depletion region (given by the condition n = p) to the right edge (given by the condition $p = N_A - 10\%$). We see that, indeed, at low voltages, this current shows a linear dependence on V, whereas at higher voltages, the current depends increasingly exponentially on V, as expected by the basic model. However, comparing Figs. 12 with 9, it is visible that this current contribution is about three orders of magnitude smaller than that leading to the departure from the superposition principle. Hence, in this idealized model, recombination in the depletion region does not contribute significantly to the departure from the superposition principle. However, this may change if real industrial solar cells without edge passivation are considered, in particular, cells made from multicrystalline silicon material. In these cells, due to extended defects crossing the p-n junction, the depletion region recombination current is orders of magnitude higher than predicted by PC1D and may show an ideality factor larger than two; see [1]. It can be expected that in such cases, the effect of a voltage-dependent recombination in the depletion region described previously may lead to significant illumination-dependent contributions both to R_p and J_{02} , as it has been measured, e.g., in [7].

IV. DISCUSSION

In this contribution, an alternative one-diode model is introduced, which allows a more realistic description of solar cells under illumination. In particular, this model provides analytic expressions for the implied voltage in the bulk, which are useful for a quantitative analysis of PL imaging experiments. In the past, such experiments have been evaluated by subtracting a PL image taken at zero bias from each of the other PL images. The simulations performed in this contribution show that this measure is justified only in the low bias range, where the influence of the diffusion resistance introduced in this contribution is significant. At least for biases approaching $V_{\rm oc}$, this measure is actually wrong, since then, also under illumination, the implied voltage basically equals the local voltage at the p-n junction, and there is no diffusion-limited current toward the p-n junction. On the other hand, since the luminescence signal is very high at high voltages, the error made by subtracting the $J_{\rm sc}$ image is very small. Thus, also in the light of this theory, the method of subtracting a V = 0 PL image is correct, as long as the lifetime is independent from the injection intensity, as also assumed here. Note that the current extracted from a solar cell is a measure of the carriers that do not recombine. According to (10), the bulk recombination rate also increases in this theory under illumination exponentially with $V_{\rm loc}$, as in the case of EL imaging. Hence, subtracting the recombination-induced luminescence at $V_{\rm loc} = 0$ leads to conditions similar to EL imaging. However, whenever an injection-dependent lifetime shall be considered, the basic theory introduced here should be applied, since it provides an explicit expression for the implied voltage, which is then governing the lifetime. In the previous PL evaluation method, the implied voltage does not appear at

Care must be taken also for adapting the results of this contribution to PL imaging experiments employing a silicon detector. This detector preferentially detects radiation from the uppermost bulk region, which contains the electron drift region, where the bulk electron concentration is at low biases significantly below the electron concentration in the center of the bulk. Here, the electron concentration is depth-dependent lying between (13) and (3). However, for InGaAs detector-based PL experiments, where light from the whole depth of the bulk is detected, this theory should be directly applicable.

According to the knowledge of the author, the advanced model introduced in this contribution explains for the first time the departure from the superposition principle described by Robinson *et al.* [3] in an analytical model. Although the alternative one-diode model introduced here should not significantly influence $V_{\rm oc}$ and the maximum power point of silicon solar cells, since the corresponding effects play a role only in the low-voltage regime, this model should contribute to a better physical understanding of the operation of solar cells. In particular, it should help in the quantitative interpretation of PL imaging results.

There are certainly several points that still may be improved in the proposed model. Note that the assumption of a constant carrier density across the bulk volume, even outside of the electron drift region, is quite a coarse assumption. In fact, the depthdependent reduction of $V_{\rm impl}$ due to the finite bulk diffusion length and backside recombination velocity is the reason for the weak discrepancy between the PC1D simulation of $V_{
m impl}^{
m dark}$ and $V_{
m loc}$. The weak deviation between J_{01} under illumination and that in the dark predicted by (10) is also not confirmed by the PC1D simulations. Maybe this effect is compensated in reality by a depth-dependent carrier concentration, which reduces J_{01} in the dark as well. In the present model, the influence of backside and emitter recombination is not explicitly considered. Moreover, it should be investigated how the aforementioned self-absorption of the PL signal in the case of a silicon detector influences the predictions of this model.

ACKNOWLEDGMENT

The author would like to thank J. Bauer and S. Rißland (Halle) for critically discussing this manuscript.

REFERENCES

- [1] O. Breitenstein, "Understanding the current-voltage characteristics of industrial crystalline solar cells by considering inhomogeneous current distributions," *Opto-Electron. Rev.*, vol. 21, no. 3, pp. 259–282, 2013.
- [2] T. Trupke, E. Pink, R. A. Bardos, and M. D. Abbott, "Spatially resolved series resistance of silicon solar cells obtained from luminescence imaging," Appl. Phys. Lett., vol. 90, no. 9, pp. 093506-1–093506-3, 2007.
- [3] S. R. Robinson, A. G. Aberle, and M. A. Green, "Departures from the principle of superposition in silicon solar cells," *J. Appl. Phys.*, vol. 76, no. 12, pp. 7920–7930, 1994.
- [4] (2014). [Online]. Available: http://www.pv.unsw.edu.au/info-about/ our-school/products-services/pc1d
- [5] S. Suckow, T. M. Pletzer, and H. Kunz, "Fast and reliable calculation of the two-diode model without simplifications," *Prorg. Photovolt., Res. Appl.*, vol. 22, pp. 294–501, 2014.
- [6] A. Cuevas, "Physical model of back line-contact front-junction solar cells," J. Appl. Phys., vol. 113, no. 16, p. 164502, 2013.
- [7] O. Breitenstein and S. Rißland, "A two-diode model regarding the distributed series resistance," Sol. Energy Mater. Sol. Cells, vol. 110, pp. 77–86, 2013.



Otwin Breitenstein received the Ph.D. degree in physics from the University of Leipzig, Leipzig, Germany, in 1980.

Since 1992, he has been with the Max Planck Institute of Microstructure Physics, Halle, Germany, where he investigated defects in semiconductors. Since 1999, he has been using lock-in thermography for detecting internal shunts and generally evaluating the local efficiency of inhomogeneous silicon solar cells. In 2001, he introduced this technique on a microscopic scale for isolating faults in ICs. He lectures

on photovoltaics with Martin-Luther-University, Halle, and is the author of a book on Lock-in Thermography. He has published more than 100 contributions about his research in scientific journals and about 150 contributions in international conference proceedings.